

THE DISTRIBUTION OF BURST ENERGY AND SHOCK PARAMETERS FOR GAMMA-RAY BURSTS

PAWAN KUMAR

Institute for Advanced Study, Princeton, NJ 08540; pk@ias.edu

Received 1999 December 23; accepted 2000 June 15; published 2000 July 26

ABSTRACT

We calculate the luminosity function for gamma-ray burst afterglows in some fixed observed frequency band and at some fixed elapsed time in observer frame (t_{obs}) in two models—one in which the explosion takes place in a uniform density medium and another in which the density falls off as inverse square (expected for stellar winds). For photon energies greater than about 500 eV and $t_{\text{obs}} \geq 10^3$ s, the afterglow flux is independent of interstellar medium (ISM) density and luminosity functions for wind and uniform ISM are identical. We deduce from the width of the observed X-ray afterglow distribution, 5 hr after the burst, that the FWHM of the distribution for isotropic energy in explosion and the fractional energy in electrons (ϵ_e) are each less than about 1 order of magnitude and the FWHM for the electron energy index is 0.6 or less.

Subject headings: gamma rays: bursts — gamma rays: theory

1. INTRODUCTION

The improvement in the determination of the angular position of gamma-ray bursts (GRBs) by the Dutch-Italian satellite *BeppoSAX* has led to the discovery of extended emission in lower energy photons lasting for days to months, which has revolutionized our understanding of GRBs (Costa et al. 1997; van Paradijs et al. 1997; Bond 1997; Frail et al. 1997). The afterglow emission was predicted prior to their actual discovery by a number of authors based on the calculation of synchrotron emission in a relativistic external shock (Paczynski & Rhoads 1993; Mészáros & Rees 1993; Katz 1994; Mészáros & Rees 1997). The afterglow observations have been found to be in good agreement with these theoretical predictions (Sari 1997; Vietri 1997a; Waxman 1997; Wijers, Rees, & Mészáros 1997).

The medium surrounding the exploding object offers some clue as to the nature of the explosion. Vietri (1997b) and Chevalier & Li (1999a, 1999b), in two very nice recent papers, have offered evidence that some GRB afterglow light curves are best explained by a stratified circumstellar medium, which suggests the death of a massive object as the underlying mechanism for gamma-ray burst explosions, as was suggested by Paczynski (1998) and Woosley (1993). Possible further evidence in support of such a model has come from the flattening and reddening of afterglow emission, a few days after the burst, in optical wavelength bands (e.g., Bloom et al. 1999; Castro-Tirado & Gorosabel 1999; Reichart 1999; Galama et al. 1999).

The goal of this Letter is to explore the afterglow flux in different models, uniform interstellar medium (ISM) as well as stratified medium, and compare it with observations in a statistical sense, as opposed to comparison with individual GRBs as carried out by Chevalier & Li (1999b). We will use this statistical comparison to constrain various physical parameters that determine the afterglow luminosity such as the energy E , the fractional energy in electrons (ϵ_e) and magnetic field (ϵ_B), the electron energy index p , and the circumstellar density n .

In the next section, we discuss the afterglow flux and its distribution and compare it with observations.

2. AFTERGLOW FLUX AND ITS DISTRIBUTION

Consider an explosion that releases an equivalent of isotropic energy E in a medium in which the density varies as Ar^{-s} ; r

is the distance from the center of the explosion, and A is a constant. The deceleration radius r_d , at which the shell starts to slow down as a result of sweeping up the circumstellar material and the deceleration time T_{da} in the observer frame are given by

$$R_{\text{da}} = \left[\frac{(17 - 4s)E}{2\pi c^2 A \Gamma_0^2} \right]^{1/(3-s)}, \quad T_{\text{da}} = \frac{R_{\text{da}}}{4\beta c (\Gamma_0/2)^2}, \quad (1)$$

where Γ_0 is the initial Lorentz factor of the ejecta and $\beta \approx 1$ is a constant.

For $R \gg R_{\text{da}}$, the time dependence of the shell radius and the Lorentz factor can be obtained from the self-similar relativistic shock solution given in Blandford & McKee (1976):

$$\frac{R(t_{\text{obs}})}{R_{\text{da}}} \equiv X = t_1^{1/(4-s)}, \quad \Gamma(t_{\text{obs}}) = \frac{\Gamma_0}{2} t_1^{-(3-s)/(8-2s)}, \quad (2)$$

where $t_1 = t_{\text{obs}} (1+z)^{-1} T_{\text{da}}^{-1}$.

The magnetic field and the electron thermal Lorentz factor behind the forward shock vary as

$$B = B_{\text{da}} \epsilon_B^{1/2} t_1^{-3/(8-2s)}, \quad \gamma_e = \epsilon_e \left(\frac{m_p}{m_e} \right) \frac{\Gamma}{2^{1/2}}, \quad (3)$$

where $B_{\text{da}} = [2(17 - 4s)E/\Gamma_0^2 R_{\text{da}}^3]^{1/2}$ is the equipartition magnetic field and ϵ_B and ϵ_e are the fractional energies in the magnetic field and the electrons, respectively.

Using these results, we find that the peak of the synchrotron frequency (ν_m) and the cooling frequency (ν_c), in the observer frame, are

$$\nu_m = \nu_{m,\text{da}} \epsilon_B^{1/2} t_1^{-3/2}, \quad \nu_c = \nu_{c,\text{da}} \epsilon_B^{-3/2} t_1^{(3s-4)/(8-2s)}, \quad (4)$$

where

$$\nu_{m,\text{da}} = \frac{1}{32\pi^2} \frac{q B_{\text{da}} m_p^2}{c m_e^3}, \quad \nu_{c,\text{da}} = \frac{9\pi}{42^{1/2}} \frac{m_e q c^3 \Gamma_0^3}{\sigma_T^2 B_{\text{da}}^3 R_{\text{da}}^2}. \quad (5)$$

The synchrotron self-absorption frequency (in the observer

frame) is given by

$$\nu_A = \left(\frac{27^{1/2} m_e c^2 \sigma_T A R_{\text{da}}^{1-s} B_{\text{da}} \Gamma_0}{64 \pi q m_p^2} \right)^{3/5} \epsilon_e^{-3/5} \epsilon_B^{3/10} \times t_1^{-0.3(4+s)/(4-s)} [\min(\nu_m, \nu_c)]^{-1/5}. \quad (6)$$

The energy flux at the peak of the spectrum is given by

$$f_{\nu_p} = \frac{27^{1/2}}{32 \pi} \left(\frac{m_e \sigma_T c^2}{q m_p d_L^2} \right) A \Gamma_0 B_{\text{da}} R_{\text{da}}^{(3-s)} \epsilon_B^{1/2} (1+z) t_1^{-s/(8-2s)}, \quad (7)$$

where $\nu_p = \min\{\nu_m, \nu_c\}$, i.e., for $\nu_m > \nu_c$ the peak occurs at ν_c instead of at ν_m .

The equations for $s = 2$ are as in Chevalier & Li (1999a, 1999b) and are given here for easy reference. The flux at an arbitrary observed frequency ν can be calculated following Sari, Piran, & Narayan (1998) in terms of f_{ν_p} , ν_m , ν_c , and ν_A . For the particularly important case of ν greater than ν_m and ν_c , the observed flux is

$$\begin{aligned} f_\nu &= f_{\nu_p} \nu_c^{1/2} \nu_m^{(p-1)/2} \nu^{-p/2} \\ &= \frac{3^{2.5} c^5}{\nu^{p/2} d_L^2} \left(\frac{q m_p^2}{m_e^3} \right)^{(p-2)/2} \frac{\epsilon_e^{p-1}}{\epsilon_B^{(2-p)/4}} \frac{(1+z)^{(3p+2)/4}}{t_{\text{obs}}^{(3p-2)/4}} \\ &\quad \times \left[\frac{(17-4s)E}{2^{10} \pi^2 c^5} \right]^{(p+2)/4}. \end{aligned} \quad (8)$$

Note that the flux does not depend on the circumstellar density parameters A and s when $\nu > \nu_c$, except through an unimportant multiplicative factor $(17-4s)^{(p+2)/4}$. The derivation of the above equation assumed that the shell is optically thin and the inverse Compton scattering does not contribute significantly to f_ν (see Panaitescu & Kumar 2000 for a more accurate calculation). Moreover, we assume spherical shell evolution which is applicable for jets as well so long as the jet opening angle is larger than Γ^{-1} —a condition that is satisfied for the observed GRB jets for about a day.

The frequencies $\nu_m/(\epsilon_e^2 \epsilon_B^{1/2})$, $\nu_c \epsilon_B^{3/2}$, and ν_A are shown in Figure 1. The afterglow flux for the uniform ISM and the wind models differ only when $\nu < \nu_c$. Since the cooling frequency decreases with time for the uniform ISM model and increases with time for the wind model, one of the best ways to distinguish between these models is by observing the behavior of the light curve at early times, typically less than a day, at frequencies below ν_c . The predictions and comparison of GRB light curves for the two models is discussed in some detail in a separate paper (Panaitescu & Kumar 2000). Here we turn our attention to the statistical property of the afterglow light curve in the two models.

2.1. Afterglow Flux Distribution Function

The distribution function for GRB afterglow flux $P(L_\nu, t_{\text{obs},g})$ at a frequency ν and time $t_{\text{obs},g}$ is the probability that the afterglow luminosity (isotropic) is L_ν at time $t_{\text{obs},g}$ after the explosion; ν , $t_{\text{obs},g}$, and L_ν are measured in the rest frame of the host galaxy.

The width of $P(L_\nu, t_{\text{obs},g})$ is a function of the width of the distribution function for \bar{E} , ϵ_e , ϵ_B , A , and p . Assuming that all these variables are independent Gaussian random variables the standard deviation for $\log(L_\nu)$, σ_{L_ν} , can be obtained from equation (8), when $\nu > \nu_c$ and $\nu > \nu_m$, and is given by

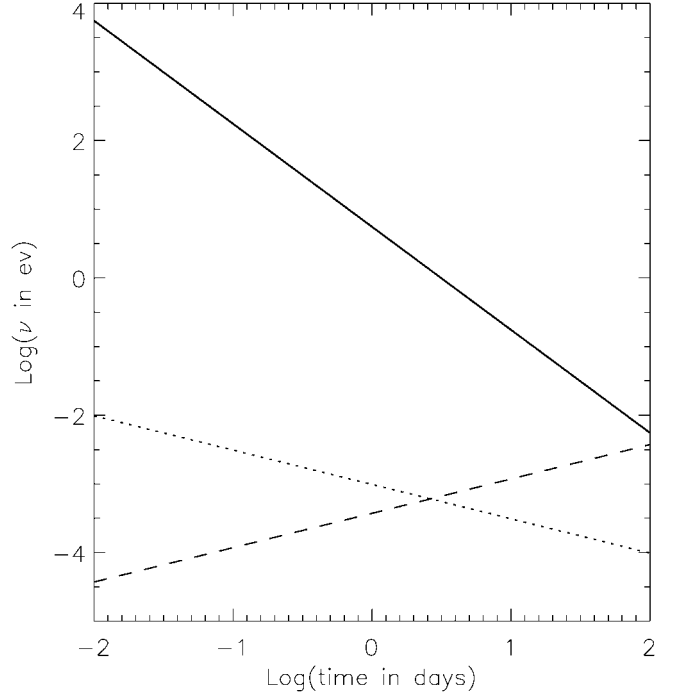


FIG. 1.—Several different frequencies, in electron volts, as a function of time in observer frame. The solid line is the peak synchrotron frequency for $\epsilon_B = 1$ and $\epsilon_e = 1$ for the wind model, i.e., $\nu_m/(\epsilon_B^{1/2} \epsilon_e^2)$ for $s = 2$; ν_m for uniform interstellar medium is larger by a constant factor of 1.374. The dotted curve is the cooling frequency $\nu_c \epsilon_B^{3/2} n_0$ for uniform ISM (n_0 is particle number density in the ISM). The dashed curve is $\nu_c \epsilon_B^{3/2} A_*^2$ for the wind model (A_* is the baryon density in the wind in units of $5 \times 10^{11} \text{ g cm}^{-3}$). The energy in the explosion E has been taken to be 10^{52} ergs and $p = 2.5$.

tion (8), when $\nu > \nu_c$ and $\nu > \nu_m$, and is given by

$$\sigma_{L_\nu}^2 = \left(\frac{p+2}{4} \right)^2 \sigma_E^2 + (p-1)^2 \sigma_{\epsilon_e}^2 + \eta \sigma_p^2 + \left(\frac{p-2}{4} \right)^2 \sigma_{\epsilon_B}^2, \quad (9)$$

where

$$\eta = \frac{1}{16} \left[2 \log \left(\frac{q m_p^2}{m_e^3} \right) + \log \left(\frac{17 \bar{\epsilon}_e \bar{\epsilon}_B^4 \bar{E}}{2^{10} \pi^2 c^5 \nu^2 t_{\text{obs},g}^3} \right) \right]^2, \quad (10)$$

$\bar{\epsilon}$ and \bar{E} are the mean values of ϵ and E , and σ_E , σ_{ϵ_e} , σ_{ϵ_B} , and σ_p are the standard deviation for $\log E$, $\log \epsilon_e$, $\log \epsilon_B$, and p , respectively; the η 's for X-ray (10 keV) and optical (2.5 eV) photons are shown in Figure 2.

The standard deviation of the flux in the 2–10 keV band at 5 hr after the burst (σ_{L_ν}) is observed to be ~ 0.58 (Kumar & Piran 2000). This result was based on seven bursts with known redshifts. Recent work of T. Piran & D. Band (2000, in preparation) uses a larger sample and more sophisticated analysis and yields essentially the same width for the X-ray afterglow luminosity function. It should be pointed out that although X-ray afterglows have been detected for almost all 27 *BeppoSAX* bursts, the selection effect for X-ray afterglow observations is difficult to quantify, and its possible effect on the determination of σ_{L_ν} is unclear. It is straightforward to redo the following analysis and determine σ_E , σ_{ϵ_e} , etc. more precisely when an accurate value for σ_{L_ν} for a much larger sample of GRBs is available from *HETE II* and *Swift*.

Figure 1 shows that 2–10 keV energy band is above ν_c and ν_m so long as $\epsilon_B > 10^{-4}$ and the density of the surrounding

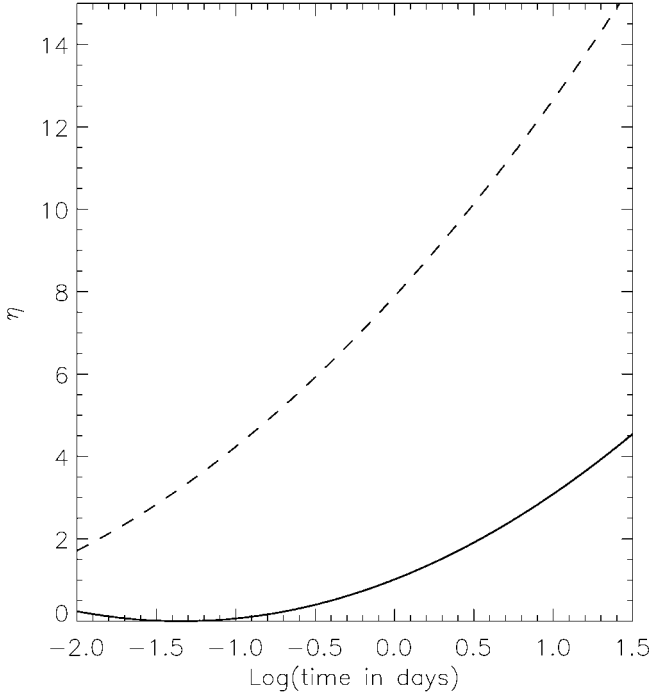


FIG. 2.— η as defined in eq. (10) is shown as a function of time for two different frequencies—2.5 eV (*solid curve*) and 10 keV (*dashed curve*). We took $E = 10^{52}$ ergs, $\bar{\epsilon}_e = 0.1$, and $\bar{\epsilon}_B = 0.03$ for these calculations.

medium is not too small. Moreover, $\eta = 5$ for this energy band (see Fig. 2), from which we obtain an upper limit on σ_p of 0.26 and the FWHM of the distribution for p to be less than about 0.6. We note that the electron energy index p lies between 2 and 3 for supernovae remnants (see Chevalier 1990; Weiler et al. 1986), and Chevalier & Li (1999b) point out that the range in p for GRB afterglows is at least ~ 2.1 – 2.5 .

We can use the variation of η with time or ν (see Figs. 2 and 3) to obtain σ_p from the observed variation to the width of σ_{L_ν} when a larger sample of GRB afterglows is available; this is equivalent to the determination of p from light curve and spectral slope.

The fractional energy in magnetic fields is highly uncertain and could vary by several orders of magnitude from one burst to another. However, so long as ϵ_B does not vary by more than 5 orders of magnitude from one burst to another, the last term in equation (9) is small and can be neglected. Equating the first two terms individually to $\sigma_{L_\nu} = 0.58$, we obtain $\sigma_E < 0.51$ and $\sigma_{\epsilon_e} < 0.39$ (for $p = 2.5$). For comparison, if the first three terms in equation (9) were to contribute equally to σ_{L_ν} , then we obtain $\sigma_E = 0.29$, $\sigma_{\epsilon_e} = 0.22$, and $\sigma_p = 0.15$. The mean values for E and ϵ_e are not well determined by this procedure (but see the discussion below); however, $\bar{E}\bar{\epsilon}_e^{4(p-1)/(p+2)}$ can be accurately obtained from the observed distribution and is $\approx 10^{52}$ ergs.

So far we have discussed a procedure for determining σ_p and a linear combination of σ_E^2 and $\sigma_{\epsilon_e}^2$ that relies on making observations in a frequency band that lies above ν_m and ν_c and hence is independent of n and s (the highly uncertain density of ISM). In order to determine σ_E and σ_{ϵ_e} separately, we need to have some knowledge of ν_c and ν_m , and therefore the result is model dependent and less certain. For instance, if the cooling and the peak synchrotron frequencies are known at some time, even if only approximately, then σ_E can be determined from the distribution of the observed flux at a frequency ν such that $\nu_c < \nu < \nu_m$. The standard deviation for $f_1 \equiv L_\nu t_{\text{obs},g}^{1/4} \nu^{1/2}$ at such

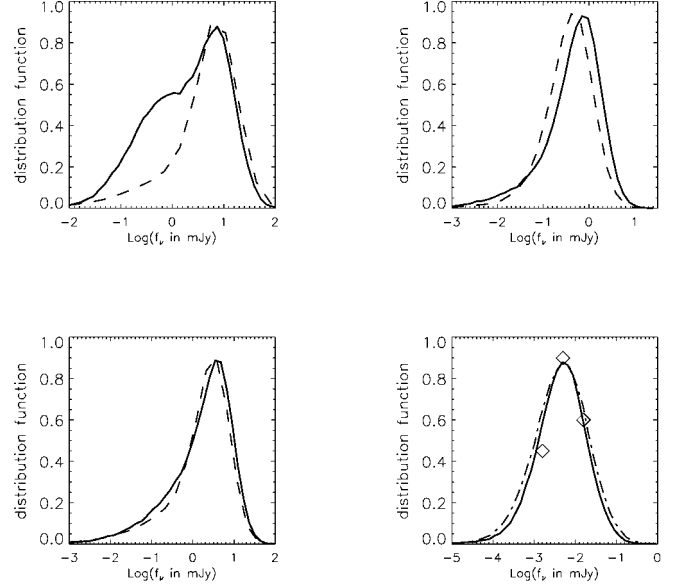


FIG. 3.—Distribution function (DF) for afterglow flux per unit frequency at photon energy of 1.0 eV, 0.1 hr after the burst (*top left panel*). The top right panel shows the DFs at photon energy of 100 eV and at 0.1 hr after the burst. The lower left panel shows DFs for photon energy of 1 eV at 1 hr after the burst. In these three cases, the solid line is for uniform ISM and dashed line is for $s = 2$. The lower right panel shows the DFs for 10 keV energy photons at 0.1 hr after the burst (*solid line*) and at 10 hr (*dash-dotted curve*) for the uniform ISM model; the dash-dotted curve has been shifted to the right by 2.4. The DF for the wind model ($s = 2$) at 10 keV energy band is identical to the uniform ISM DF at times greater than 0.5 hr except for an overall shift of the curve to lower energy by a factor of ~ 2 . For all of these calculations the FWHMs of $\log E$, $\log \epsilon_e$, $\log \epsilon_B$, A , and p were taken to be 0.8, 0.7, 3.0, 2.4, and 0.25, respectively, and the burst redshift was taken to be 1.5. Moreover, $E = 10^{52}$ ergs, $\bar{\epsilon}_e = 0.1$, $\bar{\epsilon}_B = 0.01$, and $\bar{p} = 2.3$. The diamonds in the lower panel are for bursts with known redshifts; the error bar associated with each point is much larger than the size of the symbol.

an intermediate frequency is independent of s and is given by

$$\sigma_{f_1}^2 = \frac{9}{16} \sigma_E^2 + \frac{1}{16} \sigma_{\epsilon_B}^2 \approx \frac{9}{16} \sigma_E^2. \quad (11)$$

Once σ_E is known, equation (9) can be used to determine σ_{ϵ_e} . Observations at low frequencies, i.e., $\nu < \nu_m$, ν_c , can be used to constrain σ_{ϵ_B} and σ_A , which when combined with the flux at the peak of the spectrum could be used to determine σ_{ϵ_B} and σ_A separately with the use of the following equations:

$$\sigma_{f_2}^2 = \frac{4}{(4-s)^2} \sigma_A^2 + \frac{4}{9} (\sigma_{\epsilon_e}^2 + \sigma_{\epsilon_B}^2) + \left(\frac{14-5s}{12-3s} \right)^2 \sigma_E^2 \quad \text{for } \nu < \nu_m < \nu_c, \quad (12)$$

$$\sigma_{f_3}^2 = \frac{4}{9(4-s)^2} \sigma_A^2 + \sigma_{\epsilon_B}^2 + \left(\frac{14-6s}{12-3s} \right)^2 \sigma_E^2 \quad \text{for } \nu < \nu_c < \nu_m, \quad (13)$$

and

$$\sigma_{f_4}^2 = \frac{1}{4} \sigma_{\epsilon_B}^2 + \frac{4}{(4-s)^2} \sigma_A^2 + \left(\frac{8-3s}{8-2s} \right)^2 \sigma_E^2, \quad (14)$$

where $f_1 \equiv \nu^{-1/3} L_\nu t_{\text{obs},g}^{(s-2)/(4-s)}$, $f_2 \equiv \nu^{-1/3} L_\nu t_{\text{obs},g}^{(3s-2)/(12-3s)}$, $f_3 \equiv$

$L_{\nu_p} t_{\text{obs},g}^{s/(8-2s)}$, and L_{ν_p} is the isotropic luminosity at the peak of the spectrum.

Another approach to determining the burst and shock parameters is to compare the observed flux distributions at several different frequencies and time with the theoretically calculated distributions. The latter can be easily calculated by varying E , ϵ_e , ϵ_B , A , and p randomly and solving for the flux using the equations given in the last section. Figure 3 shows a few cases of flux distribution functions for several different ν and t_{obs} . The advantage of this procedure is that it does not require observational determination of various characteristic frequencies, i.e., ν_m , ν_c , and ν_A , which is difficult to do unless we have good spectral and temporal coverage over many orders of magnitude.

It should be noted that if ν_m , ν_c , ν_A , and L_{ν_p} can be determined accurately then E , ϵ_e , ϵ_B , and A can be obtained for individual bursts as described in, e.g., Chevalier & Li (1999b) and Wijers & Galama (1999), and there is no need to resort to the statistical treatment discussed above.

3. CONCLUSION

We have described how the distribution function for GRB afterglow flux can be used to determine the width of the distribution function for isotropic energy in the explosion (E) and

the shock parameters such as ϵ_e , ϵ_B (the fractional energy in electrons and the magnetic field), p (the power-law index for electron energy), and A (the interstellar density parameter).

The afterglow flux at a frequency above the cooling and the synchrotron peak frequencies is independent of interstellar density and scales as $E^{(p+2)/4} \epsilon_e^{(p-1)} \epsilon_B^{(p-2)/4}$ for uniform ISM as well as for energy deposited in a stellar wind with power-law density stratification. Using the observed distribution of flux in 2–10 keV band, 5 hr after the burst, for seven GRBs with known redshift, we find that the FWHM of the distribution for $\log E$ is less than 1.2, $\log \epsilon_e$ is less than 0.9, and p is less than 0.6; at 5 hr the 2–10 keV band is above ν_c and ν_m .

A more accurate determination of the distribution of parameters can be carried out by comparing the theoretical and the observed distributions of afterglow flux for a larger sample of GRBs at several different frequencies which is expected from the *HETE II* and *Swift* missions.

I am indebted to Roger Chevalier for many useful discussions and for clarifying several points. I thank Alin Panaitescu, Tsvi Piran, and Bohdan Paczyński for numerous exciting discussions about gamma-ray bursts, Eliot Quataert for comments on the Letter, and an anonymous referee for comments on the X-ray afterglow selection.

REFERENCES

- Blandford, R. D., & McKee, C. F. 1976, *Phys. Fluids*, 19, 1130
 Bloom, J. S., et al. 1999, *Nature*, 401, 453
 Bond, H. E. 1997, *IAU Circ.* 6654
 Castro-Tirado, A., & Gorosabel, J. 1999, *A&AS*, 138, 449
 Chevalier, R. A. 1990, in *Supernovae*, ed. A. G. Petschek (Berlin: Springer), 91
 Chevalier, R. A., & Li, Z.-Y. 1999a, *ApJ*, 520, L29
 ———. 1999b, preprint (astro-ph/9908272)
 Costa, E., et al. 1997, *IAU Circ.* 6572
 Frail, D. A., et al. 1997, *Nature*, 389, 261
 Galama, T. J., et al. 1999, preprint (astro-ph/9907264)
 Katz, J. I. 1994, *ApJ*, 432, L107
 Kumar, P., & Piran, T. 2000, *ApJ*, 535, 152
 Mészáros, P., & Rees, M. J. 1993, *ApJ*, 405, 278
 ———. 1997, *ApJ*, 476, 232
 Paczyński, B. 1998, *ApJ*, 494, L45
 Paczyński, B., & Rhoads, J. 1993, *ApJ*, 418, L5
 Panaitescu, A., & Kumar, P. 2000, *ApJ*, submitted
 Reichart, D. E. 1999, *ApJ*, 521, L111
 Sari, R. 1997, *ApJ*, 489, L37
 Sari, R., Piran, T., & Narayan, R. 1998, *ApJ*, 497, L17
 van Paradijs, J., et al. 1997, *Nature*, 386, 686
 Vietri, M. 1997a, *ApJ*, 478, L9
 ———. 1997b, *ApJ*, 488, L105
 Waxman, E. 1997, *ApJ*, 489, L33
 Weiler, K. W., Sramek, R. A., Panagia, N., van der Hulst, J. M., & Salvati, M. 1986, *ApJ*, 301, 790
 Wijers, R. A. M. J., & Galama, T. J. 1999, *ApJ*, 523, 177
 Wijers, R. A. M. J., Rees, M. J., & Mészáros, P. 1997, *MNRAS*, 288, L51
 Woosley, S. E. 1993, *ApJ*, 405, 273